Computational Biology and Bioinformatics
2018; 6(2): 36-50
http://www.sciencepublishinggroup.com/j/cbb
doi: 10.11648/j.cbb.20180602.12
ISSN: 2330-8265 (Print); ISSN: 2330-8281 (Online)

Docking Studies for Assessment of Wound Healing Potential of Dalethyne Derivatives: An *in Silico* Approach

Kayapan Satya Dharshan

Department of Wound Care, PT Dermozone Pratama Indonesia, Jakarta, Indonesia

Email address:
article@dermozone.com, dharshan@dermozone.com

To cite this article:
Kayapan Satya Dharshan. Docking Studies for Assessment of Wound Healing Potential of Dalethyne Derivatives: An *in Silico* Approach. *Computational Biology and Bioinformatics*. Vol. 6, No. 2, 2018, pp. 36-50. doi: 10.11648/j.cbb.20180602.12

Received: October 1, 2018; **Accepted**: November 19, 2018; **Published**: December 18, 2018

Abstract: *Background*: A cascade of enzymes acting in union is involved in the natural wound healing pharmacology of humans making the process a lengthy one. This in turns necessitates new synthetic molecules effective in accelerating the wound healing process. *Objective:* The present work deals with synthetic molecules aimed at healing wounds targeting the essential enzymes involved in the wound healing process. *Method*: A series of in house synthesized dalethyne derivatives have been studied in the present work based on their ability to interact with the requisite proteins using docking methodology and degree of interactions of the molecules with each of the proteins have been determined based on their binding energy values. Subsequently, the inhibitory concentrations of the molecules were also predicted based of docking statistics. The validation of the procedure was performed based on the docking interactions of the native ligand. *Results:* The dalethyne derivatives showed effective interactions with the amino acid residues present in the active site of some of the essential proteins involved in the wound healing process accounting for the conducive effects of these molecules in the wound healing process. *Conclusion*: The present work thus provides a meaningful insight as to the structural requirements of the dalethyne derivatives that would facilitate their interaction with the receptors involved in the wound healing process such that the molecules can be efficiently formulated into a pharmaceutical dosage form.

Keywords: Dalethyne, Docking, *In Silico*, Wound Healing, Inflammation

1. Introduction

Skin is a form of natural protection against the environment and gives various essential protection functions. If the skin's integrity is disturbed, by acute or chronical wound, body will start a multistep and dynamic process at the site of the wound, which leads to healing of some parts of the tissue and the recovery of the skin protection function. The direct purpose in wound healing is to reach tissue integrity and homeostasis [1]. The natural process of wound healing consists of four phases which are overlapping but well- defined: hemostasis, inflammation, proliferation, and remodeling. Hemostasis happens to the wound as platelet aggregation which leads to blood clotting [2]. Inflammation phase includes blood cell migration, such as phagocytic neutrophil and macrophages, to the wound site [3]. Phagocyte will initially eliminate unknown particle and then will release cytokine to promote fibroblast migration and proliferation near the end of the inflammation phase [4]. Wound reepithelization is started in several hours after the wound appeared and is a part of proliferative phase [5], marked with the formation of new blood vessels (angiogenesis or neovascularization), which redefine the perfusion to keep the new tissue intact and also facilitate deposition of extracellular matrix protein fragment such as collagen fiber and granulation tissue. The last phase involves collagen remodeling and scar formation. The optimal wound healing agent will protect the tissue from bacterial infection, reduce inflammation, and induce cell proliferation to help with the reconstruction of the damaged tissue [6]. It will ideally act as antioxidant because the free radical is considered as the main cause of inflammation in the wound healing process [7].

Proper healing of wounds, arising either from injury or from diabetes, using a suitable medication poses a severe problem over the ages. Various herbal products have been used since long time for wound healing. It has been reported that bandages and dressings soaked in natural honey keep the

wound clean and stimulate the healing. Colloidal silver and Chinese herbal applications have been found to exert positive effects on faster healing [8, 9]. Fatty acids have been shown to have intense effects on wound healing and infections [10]. However, the design and modeling of fast acting synthetic drugs for the healing of chronic wounds have grabbed much attention of the current generation medicinal chemist. A great deal of effort has been given for the identification of new drug molecules that are effective in healing chronic wounds of varied nature. Current research in this field have largely addressed the *in silico* methodology for design of new synthetic molecules having improved therapeutic efficacy with a reduced toxicity profile. *In silico* technique [11] ensures prediction of the activity profile of untested molecules based on cheminformatic tools. Among the various cheminformatic tools, docking concepts [12] are now being widely employed for identifying receptor based interaction of untested molecules in comparison to a docked ligand of known activity profile. The ligand-receptor based interactions obtained from docking studies provide a quantitative as well as qualitative insight for the identification of the essential molecular attributes of the ligand molecules for showing improved activity profile.

The wound healing potential of various natural extracts have been studied by different groups of authors. Singh et al. [13] reported *in silico* and *in vivo* evidences employing MMPs as molecular targets for wound healing by *Musa sapientum*. The work reported the role of leucocyanidin, in wound healing by *in silico* methods. In the *in-silico* study, leucocyanidin was taken for evaluation as MMP inhibitor by molecular docking. Molecular docking showed that leucocyanidin was able to inhibit all selected MMPs. Incerti et al. [14] reported studies related to synthesis, biological evaluation and docking analyses for a series of 4-thiazolidinone derivatives as MMP inhibitors in tissue damage. The aim of the study was to verify their effectiveness to affect the inflammatory/oxidative process in which free oxygen and nitrite (ROS and RNS) radicals, inflammatory mediators, such as nuclear factor κB (NF-κB), and matrix metalloproteinases (MMPs) are involved. Docking studies of all the compounds were performed in order to explore their binding mode at the MMP-9 protein. Islam et al. [15] reported virtual screening studies for potential COX-inhibiting constituents from *Mimosa pudica.* The authors reported that the active compounds of *Mimosa pudica* revealed their potentiality to inhibit COX by molecular docking analysis and thus were reported to exert anti-inflamatory action. In this context, the present work has been performed to determine the wound healing potential of synthetic molecules based on their binding ability to the receptors involved in the wound healing pharmacology. Further evaluation of wound healing potential of synthetic molecules is favoured over the natural molecules due to the ease of formulation in case of synthetic molecules.

Dalethyne [16] is a content of olive oil. The novel compound dalethyne is a combination of four key compounds of peroxide, anisidine, iodine and aldehyde obtained from a process of fatty acid segregation using high-defined oxygen; that brings functions as anti-microbial, fungicidal and virucidal. Investigations have revealed that dalethyne reduces inflammation in mice and accelerate wound healing [17]. The present study focuses on the efficacy and tolerability of the dalethyne derivatives in controlling the wound related pharmacology of human beings subsequently facilitating the procedure of healing of the wound. For the present work, a series of in-house synthesised compounds have been considered and their subsequent binding interactions with specific proteins (identified to play crucial role in the wound pharmacology) have been analysed based on docking studies. The efficacy of the molecules to facilitate wound healing has been addressed in the present work.

2. Method and Materials

The present work relates to the assessment of the wound healing potential of a series of dalethyne derivatives, which have been synthesised in house, based on *in silico* analyses of the binding interactions of the compounds with specific receptors that play crucial role in the pharmacology of the wound healing process. The structures of the compounds that have been employed for the present work are provided in Table 1. The protein-ligand complex considered for the present study was selected from the protein data bank based on its resolution and specificity. The reported ligand has been used as the reference for determining the wound healing potential of the dalethyne derivatives. Validation of the docking statistics has been performed with respect to the binding interactions of the docked ligand.

Table 1. *Structures of the 18 dalethyne derivatives.*

Sl. No.	Name	Structure	No.	Name	Structure
1	Metil pelargonat $C_{10}H_{20}$	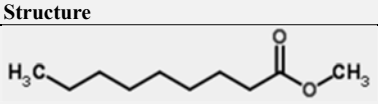	10	Metil palmitat $C_{17}H_{34}O_2$	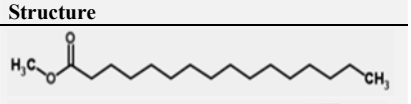
2	Metil kaparat $C_{11}H_{22}$	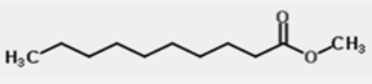	11	Metil linoleat $C_9H_{34}O_2$	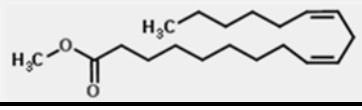

Sl. No.	Name	Structure	No.	Name	Structure
3	Metil azela aldehidate $C_{10}H_{10}O_3$		12	Metil oleat $C_{19}H_{36}$	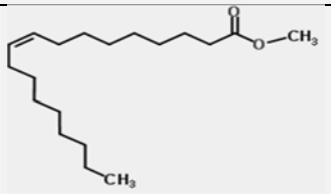
4	Dimetil suberat $C_{10}H_{18}O_4$	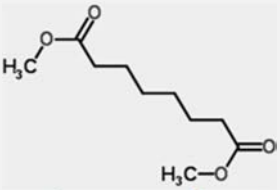	13	Metil 8-oktadekoat $C_{19}H_{36}O_2$	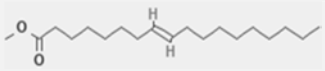
5	Metil 6,6-dimetoksi oktanoat $C_{11}H_{22}O_4$		14	Metil stearat $C_{19}H_{38}O_2$	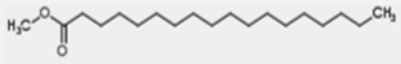
6	Dimetil azelat $C_{11}H_{20}O_4$		15	Metil 2 oktil siklopropanookta noat $C_{20}H_{38}O_2$	
7	Metil 6.6 dimetoksi oktanoat		16	Metil 11-eikosanoat $C_{21}H_{40}O_2$	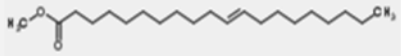
8	Metil miristat $C_{15}H_{30}O_2$		17	Metil eikosanoat $C_{21}H_{42}O_2$	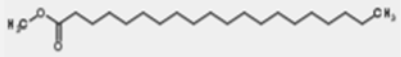
9	Dimetil undekadinoat $C_{12}H_{24}O_2$		18	Metil dokosanoat $C_{23}H_{46}O_2$	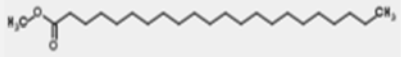

2.1. In Silico Tools and Molecular Docking

All the inhouse synthesised molecules that were considered for the present study were drawn using Marvin Sketch [18], in 2D and 3D formats. Subsequently the structures were exported as .pdb file format and were prepared using the 'Ligand Preparation Module'. The X-ray crystallographic structures of all the receptors involved in the process of wound healing were downloaded from protein data bank [19] in .pdb file format. The selection of the crystallographic structure was done based on their resolution. The proteins thus selected were complexed with the native ligand. Subsequently, the native ligand was removed from the receptor and was prepared in a process similar to that followed for the preparation of the dalethyne derivatives. The receptor thus separated from the ligand was prepared using the Autodock software [20]. Water molecules were removed from the receptor structure and the polar hydrogens were added. The Gasteiger charges were calculated for the receptor and the protein structure thus obtained was saved .pdbqt format. The docked position of the native ligand was marked as the active site of the receptor with optimized grid box size and centered grid position. For the purposes of docking, the ligands and the receptor thus prepared were fed as inputs into the Autodock software. The docking output file saved as .dlg file format was analysed using Autodock and the binding energies of the moles and their K_i values were calculated. Analysis and visualization of the receptor-ligand complex resulting from the docking studies was done by using Ligplus and PyMOL software [21].

2.2. Docking Methodology

Docking [12] refers to an *in-silico* methodology for drug design that facilitates identification followed by quantization of protein-ligand interaction. Various types of software are available for performing the docking procedure with varying types of molecular modeling algorithms. In the present work, the Autodock software has been utilized for performing the docking process. The methodology involved in the docking statistics allows identification of the ideal ligand binding with the receptor molecule. The degree of interactions between the ligands and the receptors are determined based on calculation of free energies of interaction. Molecules with lower values of free energy for binding to the receptor are considered to be ones with increased potential for interacting with the receptor. Moreover, the validation of the docking procedure has been performed based on the binding interactions of the native ligand re-docked into the receptor structure. Additionally, the dissociation constant of the molecules from the receptor is noted based on the k_i values. The docking interactions bewtween the in house synthesised dalethyne derivatives and each of the receptors involved in the process of wound healing has been determined and validated based

on the native ligand.

2.3. Pharmacology Involved in the Wound Healing Process

2.3.1. Inflammation Phase

Inflammation is the second important phase in the wound healing process, which is often considered as the first step in the optimal skin regeneration [5]. Uncontrollable inflammation response could cause unwanted effect that could damage the tissue, as we could see in the case of inflammation disturbance such as rheumatoid arthritis. Considering that the tissue wound could cause acute inflammation, inflammation control is very expected and could optimize the wound healing process.

I Compound docking with p50 NF-κB

NF-(κ)B (nuclear factor kappa-light-chain-enhancer of activated B cells), is a transcription factor that organize many genes which are involved in the initiation of the inflammation response. NF-κB could be activated by various stimulus such as microbial and virus product, pro-inflammation cytokine, T-cell and B-cell mitokin, and physical and chemical pressure. NF-κB organizes expressions that could be induced by many cytokines, chemokines, adhesion molecules, acute-phase proteins, and antimicrobial peptides. Thus, most of the NF-κB inhibitors function by inhibiting activation or phosphorylation of IκB and degradation, therefore preventing the release of free NF-κB. However, approaching direct inhibition of DNA NF-κB bond by disturbing the DNA binding area in NF-κB seemed to be more effective and could be used to design specific inhibitor. Specific amino acids which are responsible for the interaction with the DNA are those that interact with residue numbers 59-71 from p50 subunit (59: Arg, Tyr, Val, Cys, Glu, Gly, Pro, Ser, His, Gly, Gly, Leu, Pro: 71), commonly referred to as DBR (DNA Binding Region). All of the synthesised compounds were docked to the receptor binding site (ID PDB: 1SVC) using Autodock 4.2. Grid has been prepared for each protein with the same center and with the grid box size set at a point distance of 0.375 Å and sized 60 x 60 x 60. The coordinates of the grid box: x=37.569; y=24.176; z=38.430).

II Compound docking with Interleukin-6

Interleukin-6 (IL-6) is a multifunctional cytokine with main role in inflammation, infection response, metabolic regulation, regenerative, and neurological process. The normal physiological concentration of IL-6 in human serum is quite low (1-5pg / mL), but it could increase significantly during infection, autoimmunity, and inflammation. IL-6 has three different epitopes: site I, site II, and site III. IL-6, site I is a complex form with non-signaling receptor, IL-6R (also known as gp80, CD126). Then, the next one is a composite epitope (called as site II) which interacts with the cytokine homology binding site of glycoprotein 130 (gp130) to produce IL-6R:IL-6:gp130 trimer. The last interaction is between IL-6 site III with the immunoglobulin activation domain gp130 from the two trimer, producing hexamerica signaling complex that will activate JAK / SAT pathway which cause inflammation. All of the studied compounds were docked to the receptor binding site (ID PDB: 1ALU) using Autodock 4.2. Grid was prepared for each protein with the same center and with the grid box size set at a point distance of 0.375 Å and sized 50 x 50 x 50. The coordinates of the grid box were identified to be x=-3.934; y=-18.113; z=3.394. Amino acid residues Leu33, Arg168, Glu172, Gln175, Ser176, Leu178, Arg179, and Ala180 located at A and D helices of the protein constitute the binding site at site I.

III Compound docking with COX-2

COX has three isoform: COX-1, COX-2, and COX-3. COX-3 recently identified in humans has been found to be involved in pain and fever mechanism. COX-2 is not usually expressed in most cells but is induced significantly as a response to the inflammation stimulus which in turn produces prostaglandins, such as prostaglandin E2 (PGE2). All of the studied compounds were docked to the receptor binding site (ID PDB: 5IKQ) of the protein using Autodock 4.2. Grid was prepared for each protein with the same center and with the grid box size which at a point distance of 0.375 Å and sized 40 x 40 x 40. The coordinates of the grid box were identified to be x=22.222; y=52.346; z=18.018.

IV Compound docking with TNF-α

TNF-α disturbs fibroblast function and an increase in TNF-α mast cell is related to vein ulcers. There is not much literature to show the possibility of TNF-α contribution in human chronic wound condition. Though TNF-α is beneficial as protection against pathogen, TNF-α is also related with the host destruction effect. The blockage of TNF-α has proven to increase collagen deposit in the research using mice; showing that this tissue cytokine has the ability to inhibit wound healing process. All of the studied compounds were docked to the receptor binding site (ID PDB: 2AZ5) using Autodock 4.2. Grid was prepared for each protein with the same center and with the grid box size set at a point distance of 0.375 Å and sized 40 x 40 x 40. The coordinate of the grid box was marked as: x=-19.259; y=74.79; z=34.032).

V Compound docking with interleukin-1β

IL-1β processing by caspase-1 through inflammation indicates the role of IL-1β in inflammation and pain during sick condition. The strategy in inhibiting the interaction at the interface of IL- 1β/IL-1RI has been recommended as the target strategy of IL-1β inhibitor. To block the interaction between IL-1β and IL-1R, IL-1β and IL-1R, complex interface analysis showed two possible interaction locations; which have been marked as sites A and B. These two IL-1β sites interacted with different domain of IL-1R. Site A consisted of residue number 11, 13-15, 20-22, 27, 29-36, 38, 126-131, 147, and 149. The critical binding residues were determined to be Arg11 and Gln15. The surface of binding site (site A) has pockets for receiving the side chain of IL-1β. Therefore, the important components of the binding energy of this site possibly originated from van der Waals contact between IL-1β and IL-1R. The second binding site (site B) has been found to consist of residue numbers 1-4, 6, 46, 48, 51, 53-54, 56, 92-94, 103, 105, 106, 108, 109, 150, and 152. The two hydrophilic residues (Arg4, Gln48, Glu51, Asn53, Lys93, Glu105, and Asn108) and hydrophobic residues (Leu6, Phe46, Ile56, and Phe150) interact with the surface of

IL-1R, therefore the binding energy at location B has been reported to be more depending on the hydrophilic and hydrophobic interactions. All of the studied compounds were docked to the receptor binding site (ID PDB: 1ITB) using Autodock 4.2. Grid has been prepared for each protein with the same center and with the grid box size was set at a point distance of 0.375 Å and sized 60 x 60 x 60. The coordinates of the grid box were marked as x=-48.729; y=3.25; z=16.546.

VI Compound docking with MMP-9

In case of acute wound, there is a balance between the activity of protease and the precipitation of extracellular matrix component (ECM). However, over-activity of metalloproteinase matrix (MMP) contributes to the development of chronical wound. Delayed healing is marked by the increase of MMP. MMP-9, in particular, has been implicated to be dynamically organized in some pathological processes. Therefore, the development of MMP inhibitor had been an interesting strategy in the process of wound healing. All of the studied compounds were docked to the receptor binding site (ID PDB: 5UE4) using Autodock 4.2. Grid is prepared for each protein with the same center and the grid box size was set at a point distance of 0.375 Å and sized 40 x 40 x 40. The coordinates of the grid box were identified as x=48.145; y=64.14; z=42.896.

2.3.2. Proliferation Phase

Proliferative phase in wound healing process involves granulation tissue formation and collagen deposition (extracellular protein matrix formation), fibroblast proliferation, epithelization, and unwanted cell apoptosis [5].

I Compound docking with FGF2/FGF2-FGFR1 complex

Fibroblast growth factor (FGF) plays important roles in various critical biological processes; such as cell proliferation, life continuity, differentiation, cell migration, morphogenesis, and angiogenesis. FGF binds tyrosine kinase receptor and heparin sulfate receptor (HS), a proteoglycan sugar component which is wide-spread in the cell and extracellular matrix surface. HS protects FGF from inactivation and facilitates FGF receptor binding, which cause biological signal and response. In the family of FGF, FGF1 and FGF2 are mostly researched. A heparin that bind FGF2 and FGFR1 acts as a stimulator of the growth factor and the heparin that binds only FGF2 acts as the signaling inhibitor by absorbing the growth factor. All of the studied compounds were docked to the receptor binding site (ID PDB: 4OEE) using Autodock 4.2. Grid has been prepared for each protein with the same center and with the grid box size set at a point distance of 0.375 Å and sized 40 x 40 x 40. The coordinates of the grid box were identified to be: x=-11.744; y=-6.027; z=-3.063). Similarly, docking of the compounds to the binding site (ID PDB: 1FQ9) of FGF2-FGFR1 complex yielded a grid box with co-ordinates of x=86.632; y=30.008; z=110.516.

II Compound docking with IGF1R

As a part of the signaling molecule class, insulin-like growth factor tyrosine kinase receptor (IGF1R) is an important element in the signaling pathway which is involved in cell growth, proliferation, and survival. All of the in-house synthesised compounds were docked to the receptor binding site (ID PDB: 2ZM3) using Autodock 4.2. Grid was prepared for each protein with same center with grid box size set at a point distance of 0.375 Å and sized 40 x 40 x 40. The coordinates of the grid box were marked as x=37.061; y=79.097; z=58.051).

III Remodeling Phase

As the last phase of wound healing process (together with remodeling), reepithelization is a strong process which recover the barrier function of epidermis [22]. TGF-β is involved with some process in wound healing: inflammation, angiogenesis stimulation, fibroblast proliferation, collagen, synthesis, and precipitation and also new extracellular matrix remodeling. Wang *et al*. [23] showed that the fibroblast extracted from the hypertrophic scar produced more mRNA and TGF-β1 protein than normal skin or fibroblast originating from normal skin. Therefore, there is a possibility that TGF-β1 has a role in hypertrophic scar formation. All of the studied compounds were docked to the receptor binding site (ID PDB: 1VJY) using Autodock 4.2. Grid was prepared for each protein with the same center and with grid box size set at a point distance of 0.375 Å and sized 40 x 40 x 40. The coordinates of the grid box were identified to be: x=-8.389; y=63.222; z=-11.861).

3. Results and Discussion

All the 18 dalethyne derivatives were assessed for their ability to facilitate wound healing by analysing their binding interactions with the various proteins that play specific roles in the different stages of the wound healing procedure in the human body. The compounds were docked to each of the different proteins and their binding interactions were assessed in comparison to the docked ligand. The binding interactions of the molecules have been determined based on their free energy values for such interaction. All the molecules of the present study were docked to each of the proteins involved in the process of wound healing. Among all, the molecules showing significant interactions with the respective proteins, when compared with the interaction of the native ligand, have been shown in the following figures.

Thus for the purpose of validation, interactions of the 18 dalethyne compounds have been compared with those of the native ligand. The activities of the studied molecules have been predicted based on their ability to dock into the active site of the receptor. The activity values of the molecules, based on the predictive potential of the molecules with different receptors associated with the wound healing process, as calculated based on the docking results are shown in Tables 2 and 3 . The prediction of the activities of the molecules has been done based on their K_i values measured in μm units referring to the 50% inhibitory constant of the molecules.

Table 2. *Binding energies and predicted activity data for the dalethyne derivative based on ligand receptor interaction in the inflammation phase.*

Sl. No.	Compound name	p50 NF-κB		interleukin-6		COX-2	
		ΔG (kcal/ mol)	Ki (μM)	ΔG (kcal/ mol)	Ki (μM)	ΔG (kcal/mol)	Ki (mM)
1	Methyl pelargonat	-5.76	59.83	-3.62	2.24	-5.21	151.72
2	Dimethyl suberat	-4.78	312.22	-3.79	1.66	-5.21	150.46
3	Methyl 6,6-dimetoksioctanoate	-4.83	286.76	-3.36	3.45	-4.41	589.20
4	Methyl kaparat	-5.57	83.03	-4.05	1.07	-5.81	54.80
5	Methyl 6,6-dimetoksioctanoate	-4.83	286.76	-3.36	3.45	-4.41	589.20
6	Methyl miristat	-5.19	156.16	-4.30	0.71	-6.11	32.97
7	Methyl azela-aldehidate	-5.02	210.66	-3.66	2.07	-5.57	81.99
8	Dimethyl azelat	-5.13	174.99	-3.98	1.20	-5.24	143.48
9	Dimethyl undekadinoat	-5.40	110.76	-3.87	1.45	-5.99	40.73
10	Methyl palmitate	-4.84	282.33	-3.02	6.08	-5.85	51.63
11	Methyl 8-octadekanoate	-6.05	36.45	-3.99	1.18	-6.49	17.60
12	Methyl 11-eikosenoat	-5.37	116.41	-3.27	3.98	-6.24	26.68
13	Methyl linoleate	-5.48	96.65	-3.81	1.62	-7.06	6.66
14	Methyl stearate	-4.77	317.18	-4.25	0.76	-6.55	15.83
15	Methyl eikosanoat	-4.19	845.38	-2.76	9.54	-6.10	33.65
16	Methyl oleate	-5.42	106.23	-3.69	1.96	-6.79	10.54
17	Methyl 2-octilcyclopropanooctane	-4.97	227.49	-3.34	4.67	-7.18	5.43
18	Methyl dokosanoat	-3.26	4110	-2.99	6.45	-6.70	11.20
19	Native ligand	-	-	-5.31	0.13	-8.39	0.71

Table 2. *Continue.*

Sl. No.	Compound name	TNF-α		IL-1β		MMP-9	
		ΔG (kcal/ mol)	Ki (mM)	ΔG (kcal/ mol)	Ki (μM)	ΔG (kcal/ mol)	Ki (μM)
1	Methyl pelargonat	-3.01	6.26	-4.19	852.64	-4.94	237.37
2	Dimethyl suberat	-3.08	5.53	-4.78	314.99	-4.97	228.32
3	Methyl 6,6-dimetoksioctanoate	-2.9	7.53	-3.92	1330	-4.78	314.52
4	Methyl kaparat	-3.22	4.35	-4.44	561.66	-5.37	114.99
5	Methyl 6,6-dimetoksioctanoate	-2.9	7.53	-4.58	437.18	-4.78	314.52
6	Methyl miristat	-3.18	4.67	-3.92	1330	-5.72	63.62
7	Methyl azela-aldehidate	-3.12	5.15	-4.64	396.99	-4.73	340.64
8	Dimethyl azelat	-3.37	3.38	-4.35	646.49	-5.07	191.66
9	Dimethyl undekadinoat	-2.95	6.83	-4.68	373.33	-5.26	140.33
10	Methyl palmitate	-2.89	7.61	-3.56	2450	-5.22	148.16
11	Methyl 8-octadekanoate	-3.41	3.15	-3.65	2100	-5.89	47.88
12	Methyl 11-eikosenoat	-2.59	12.66	-3.72	1870	-6.19	29.25
13	Methyl linoleate	-2.79	8.95	-4.16	894.97	-6.75	11.26
14	Methyl stearate	-1.99	34.7	-3.52	2.63	-5.16	165.73
15	Methyl eikosanoat	-1.72	54.48	-3.63	2200	-5.38	113.52
16	Methyl oleate	-3.5	2.73	-3.88	1440	-5.96	42.97
17	Methyl 2-octilcyclopropanooctane	-2.81	8.73	-4.2	838.2	-6.07	35.33
18	Methyl dokosanoat	-1.91	40.04	-3.3	3650	-4.59	433.73
19	Native ligand	-6.64	0.013	-	-	-8.54	0.548

Table 3. *Binding energies and predicted activity data for the dalethyne derivative based on ligand receptor interaction in the proliferation and remodeling phases.*

Sl. No.	Compound name	Proliferation phase			
		FGF-2		FGF2-FGFR1 complex	
		ΔG (kcal/ mol)	Ki (mM)	ΔG (kcal/ mol)	Ki (μM)
1	Methyl pelargonat	-3.14	4.96	-4.33	667.68
2	Dimethyl suberat	-3.78	1.68	-4.52	488.61
3	Methyl 6,6-dimetoksioctanoate	-3.52	2.63	-4.40	596.54
4	Methyl kaparat	-3.03	6.04	-4.85	279.79
5	Methyl 6,6-dimetoksioctanoate	-3.52	2.63	-4.40	596.54
6	Methyl miristat	-2.52	14.13	-4.48	521.51
7	Methyl azela-aldehidate	-3.13	5.07	-4.67	374.65
8	Dimethyl azelat	-3.57	2.42	-4.86	274.60
9	Dimethyl undekadinoat	-3.06	12.71	-4.72	349.67
10	Methyl palmitate	-1.71	55.82	-5.17	161.24
11	Methyl 8-octadekanoate	-1.53	76.04	-4.92	248.23

Sl. No.	Compound name	Proliferation phase			
		FGF-2		FGF2-FGFR1 complex	
		ΔG (kcal/ mol)	Ki (mM)	ΔG (kcal/ mol)	Ki (μM)
12	Methyl 11-eikosenoat	-1.27	116.42	-3.79	1650
13	Methyl linoleate	-1.92	39.25	-4.59	431.38
14	Methyl stearate	-1.68	58.21	-4.40	593.80
15	Methyl eikosanoat	-1.11	153.10	-4.53	481.10
16	Methyl oleate	-1.30	112.14	-4.85	279.89
17	Methyl 2-octilcyclopropanooctane	-1.72	54.49	-4.70	358.88
18	Methyl dokosanoat	-0.20	718.31	-4.97	228.06
19	Native ligand	-10.87	10.85	-11.95	0.0018

Table 3. *Continued.*

Sl. No.	Compound name	Proliferation phase		Remodeling phase	
		IGFR1		TGF-β1	
		ΔG (kcal/ mol)	Ki (mM)	ΔG (kcal/ mol)	Ki (μM)
1	Methyl pelargonat	-3.94	1.29	-5.20	154.30
2	Dimethyl suberat	-3.45	2.95	-5.09	185.48
3	Methyl 6,6-dimetoksioctanoate	-3.49	2.76	-4.74	332.69
4	Methyl kaparat	-4.01	1.14	-5.64	73.07
5	Methyl 6,6-dimetoksioctanoate	-3.49	2.76	-4.74	332.69
6	Methyl miristat	-3.74	1.83	-5.89	48.40
7	Methyl azela-aldehidate	-3.68	2.02	-5.06	195.66
8	Dimethyl azelat	-3.59	2.35	-5.37	115.59
9	Dimethyl undekadinoat	-3.96	1.26	-5.21	151.72
10	Methyl palmitate	-3.79	1.67	-5.40	150.46
11	Methyl 8-octadekanoate	-3.74	1.80	-4.41	589.20
12	Methyl 11-eikosenoat	-4.06	1.06	-5.19	156.16
13	Methyl linoleate	-4.50	0.502	-5.02	210.66
14	Methyl stearate	-3.78	2.14	-5.13	174.99
15	Methyl eikosanoat	-3.57	2.41	-4.77	317.18
16	Methyl oleate	-4.24	0.781	-4.19	845.38
17	Methyl 2-octilcyclopropanooctane	-3.65	2.10	-4.78	312.22
18	Methyl dokosanoat	-3.35	3.52	-4.83	286.76
19	Native ligand	-8.99	258.78	-9.69	79.14

3.1. Inflammation Phase

The results of docking studies related to the receptors involved in the inflammation phase are provided in Table 2 and 4. Six different proteins have been found to play crucial role in the process of inflammation. The dalethyne derivatives analysed in the present study were docked to each of the 6 different proteins that account for the first step of the wound healing process, inflammation phase. In addition, the most active compounds have been further analysed based on their interaction pattern for each of the individual proteins.

Figure 1 shows the interaction pattern of the most active compounds (Compounds 1, 11 and 13) with respect to NF-κB protein. Based on the docking results (Figure 1), it was observed that the compounds exhibited activity as DNA NF-κB inhibitor. Compound no. 11 formed strong hydrogen bond with Ser243, while compound 1 indicated two weak hydrogen bonds with Hys67 and Gly68. Most of the residues which interacted with the ligand constitute the binding site of NF-κB DNA bearing residues 56, 58, 59, 61, 62, 65, 68, 143, 145, 146, 243. Figure 2 displays the pattern of interaction between the amino acid residues of the active site of Interleukin-6 and the dalethyne derivatives (compound nos. 4, 6 and 14). Based on the docking results (Figure 2), the compounds with effective interleukin-6 inhibition activity were identified. Compound nos. 4, 6 and 14 showed hydrogen bond based interactions with Arg179 and Arg182 residues of the ligand binding site of the protein indicating that compound nos. 4, 6 and 14 have similar activity as the native ligand. However, both of the native ligand and the compounds showed only little interaction as IL-6 inhibitor which is chiefly attributed to the simple structure of these compounds in comparison to the complex structure of the well-known IL-6 inhibitor (monoclonal antibody). Figure 3 represents the binding interactions between the amino acids constituting the active site of the COX protein and the active dalethyne derivatives (Compound nos. 13, 16 and 17) as well as the native ligand. Based on the docking result (Figure 3), it was observed that the compounds showed efficient activity as COX-2 inhibitor. COX-2 active site consists of three important domains: a hydrophobic pocket which is marked with Tyr385, Trp387, Phe518, Ala201, Tyr248, and Leu352. The second key domain bound by three hydrophilic amino acid residues (Arg120, Glu524, and Tyr355) which are located at the entrance of the temporary active site. The third domain is a side pocket which is marked with His90, Arg513, and Val523. From Figure 3, it can be inferred that compound no. 17 forms strong hydrogen bond with Tyr355, while

compound no. 16 also showed strong hydrogen bond interaction with theTyr385 residue of the COX-2 protein. The results indicated that compound nos. 16 and 17 showed efficient interaction with the protein. Figure 4 shows the interactions between the amino acid residues of the active site of TNF-α and compound nos. 8, 11 and 16. The ligand molecule was also re-docked into the protein active site and the binding interactions thus reported were compared with those of compound nos. 8, 11 and 16. Based on the docking results (Figure 4), it was observed that the compounds have little activity as TNFα inhibitor. TNFα active sites were marked as residue numbers of 57, 59, 60, 119-122, 151 (PDB). Compound no. 16 formed two strong hydrogen bonds with Lys98 and Tyr119, compound no. 11 also showed two strong hydrogen bonds with Lys98 and Tyr 119, and compound no. 8 showed further two hydrogen bonds with Gly121 and Tyr151. Ligand molecule also showed similar hydrogen bond interactions with at Tyr119. However, more interaction between the ligand molecule and the active site residues of the protein in comparison to the other studied compounds have been attributed to the simple structure of the dalethyne derivatives. The well-known TNFα inhibitor is monoclonal antibody, a protein with a complex structure and hence showing more interactions than the small molecules (dalethyne derivatives). The present study showed that the compounds do interact with TNFα active site and hence do not have good inhibition mark as TNFα inhibitor. Figure 5 shows docking interactions between the amnio acid residues and compound nos. 2, 7 and 8. Based on the docking results (Figure 5), it was observed that the compounds showed low activity as IL-1β inhibitor. Compound no. 2 showed three hydrogen bonds with Lys103, Met148, and Thr300; compound no. 9 showed only one hydrogen bond with Thr300; and compound no. 7 indicated two hydrogen bonds with Gly121 and Thr151. Thus, concluding that the simple structure of the compounds attributed to their reduced activity towards IL-1β, the well-known IL-1β inhibitor being a monoclonal antibody with a complex structure. The results although showed reduced interaction between the studied compounds and IL-1β inhibitor but do not showed the properties of a very good inhibitor. Figure 6 shows interactions of compound nos. 12, 13 and 17 with the active site of MMP-9. The degree of interactions of the compounds was subsequently compared with the interaction pattern of the native ligand with respect to the said protein. Based on the docking results (Figure 6), it was observed that the compounds showed efficient activity as MMP-9 inhibitor. Compound nos. 12 and 13 showed strong hydrogen bond with Arg106. The compounds could inhibit MMP-9 in degrading TIMP, gelatin, or other ECM by blocking the TIMP and gelatin binding site. Therefore, those compounds have been predicted to have the ability to fasten the wound healing process.

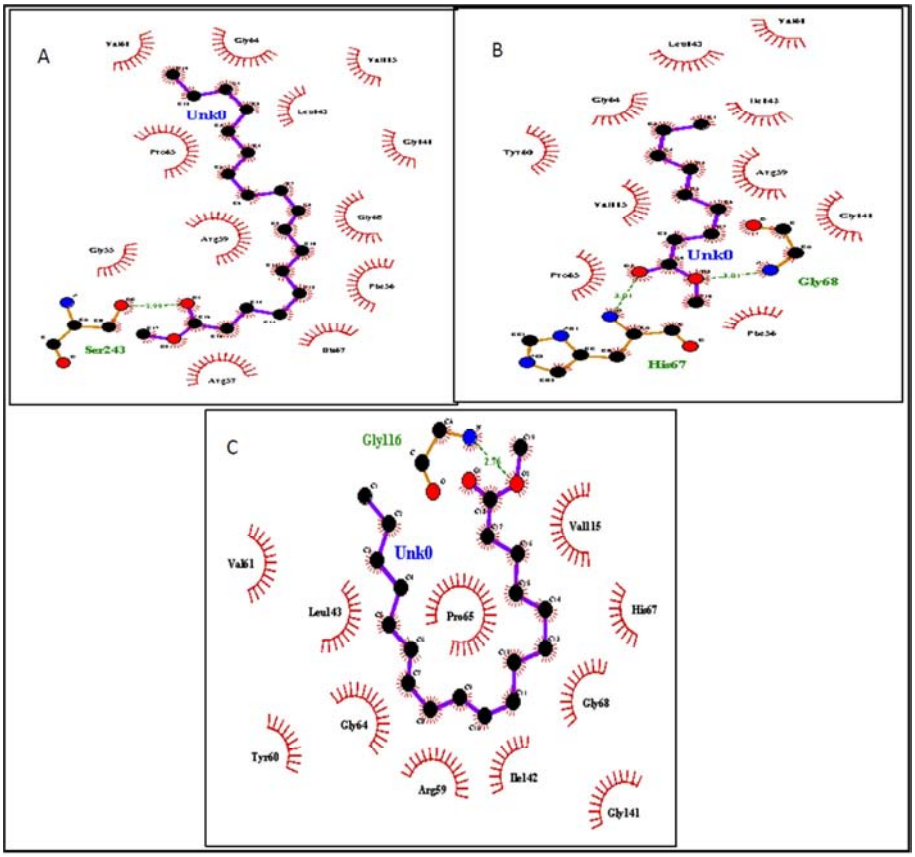

Figure 1. *2D interaction between compound with amino acid residue of NF-κB protein (A: compound number 11, B: compound number 1, C: compound number 13).*

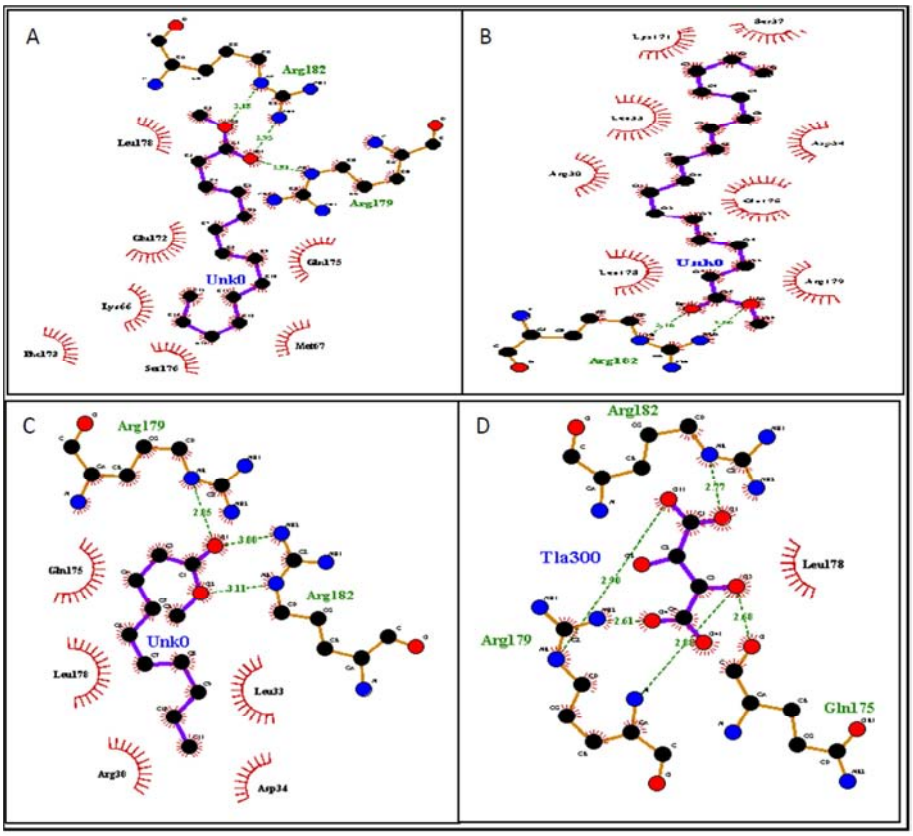

Figure 2. *2D interaction between compound and amino acid residue of Interleukin-6 (A: compound number 6, B: compound number 14, C: compound number 4, D: native ligand).*

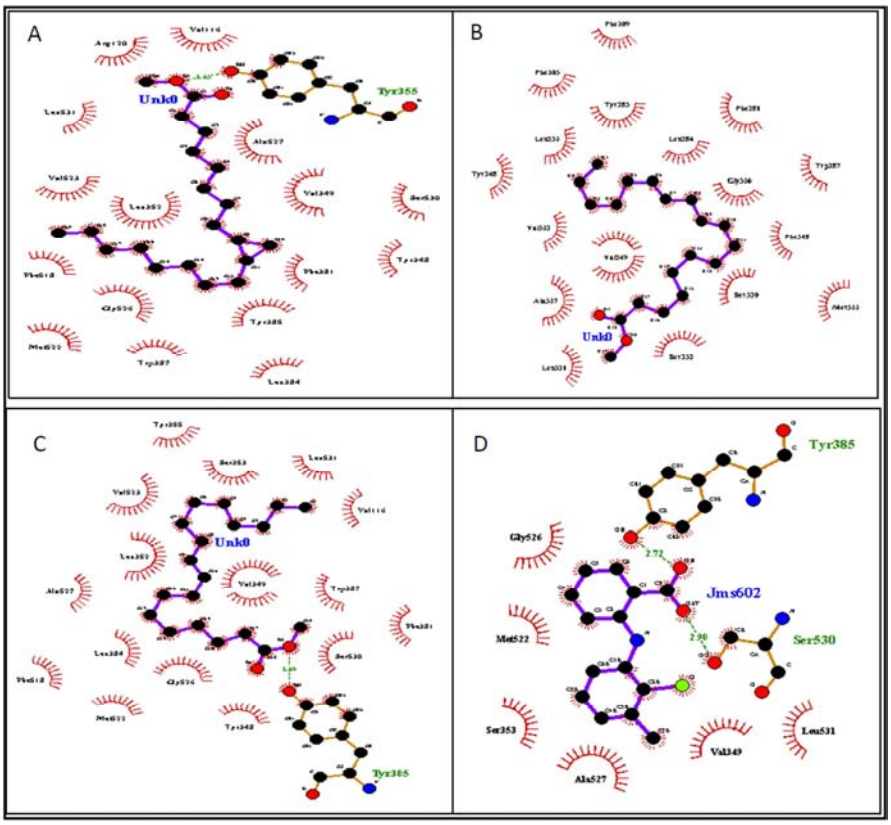

Figure 3. *2D interaction between compound with amino acid residue of COX protein (A: compound number 17, B: compound number 13, C: compound number 16, D: ligand.*

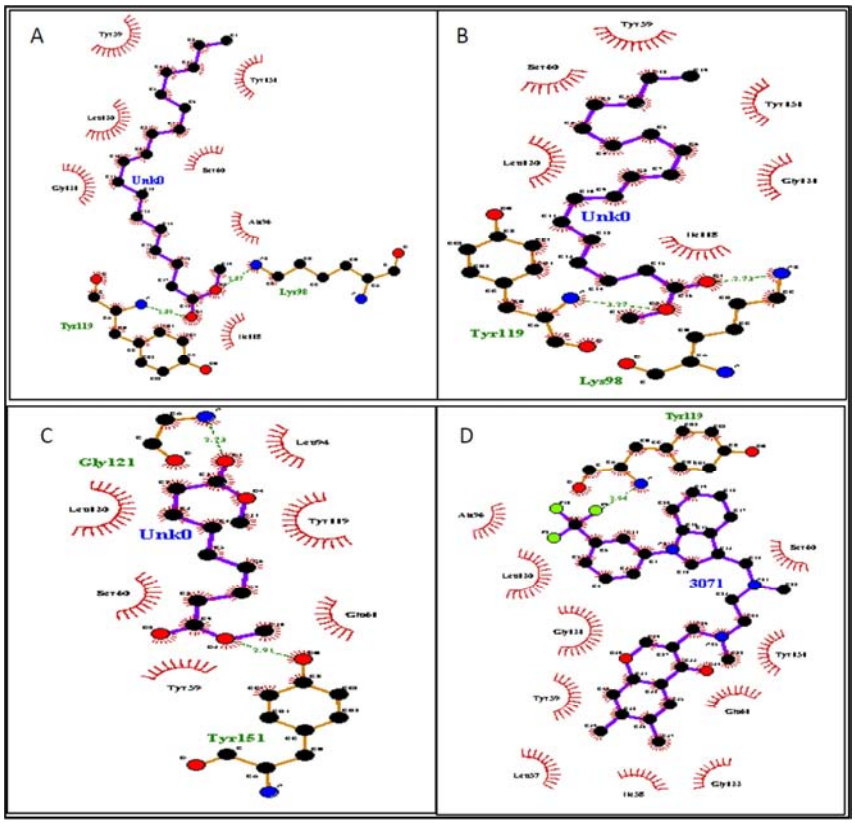

Figure 4. *Figure 10: 2D interaction between compound with amino acid residue of TNF-α (A: compound number 16, B: compound number 11, C: compound number 8, D: ligand).*

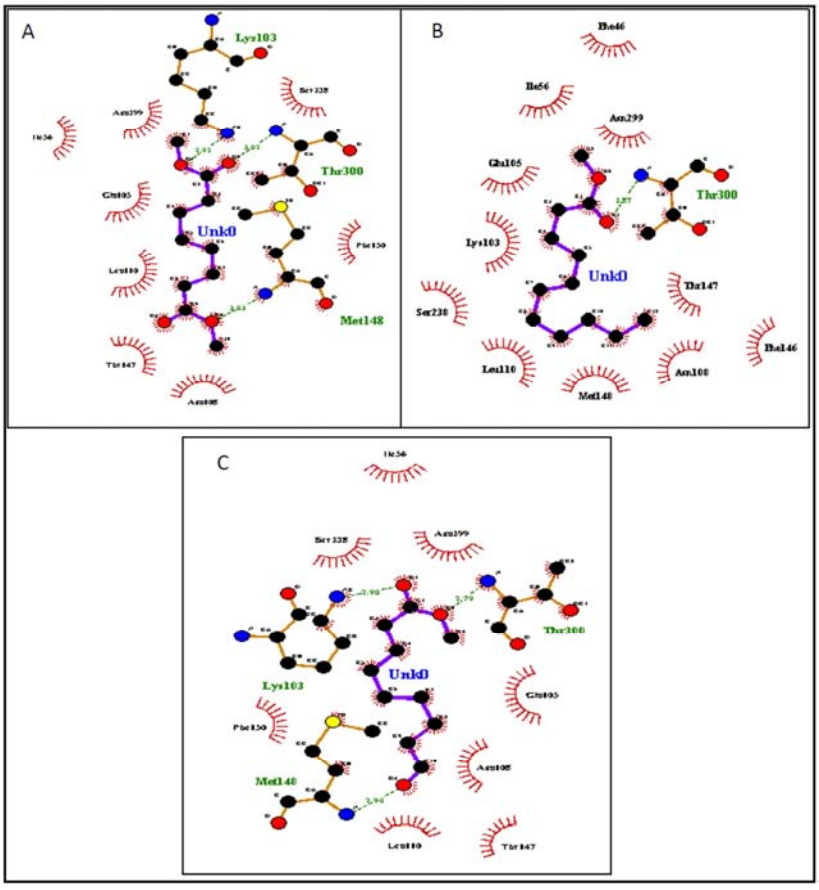

Figure 5. *2D interaction between compound with amino acid residue of IL-1β (A: compound number 2, B: compound number 9, C: compound number 7).*

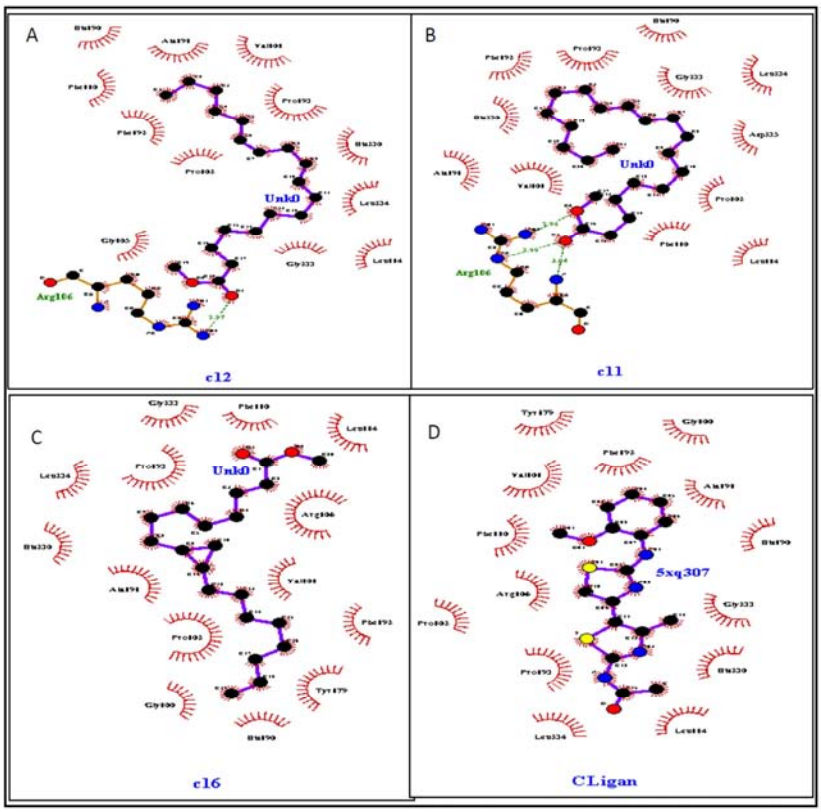

Figure 6. *2D interaction between compound with amino acid residue of MMP-9 (A: compound number 13, B: compound number 12, C: compound number 17, D: ligand).*

3.2. Proliferation Phase

The results of docking studies related to the receptors involved in the proliferation phase are provided in Table 3. This step constitutes the second phase of the wound healing process and involves the functioning to two different growth factors. Figure 7 shows the docking interactions between FGF2 factor and compound nos. 2, 3 and 8. The docking interactions of these compounds were subsequently compared to the interactions based on the docking of the native ligand to the growth factor. Based on the docking results (Figure 7), it was observed that the compound did not show activity as FGF2 inhibitor because the ΔG value were larger than -4. The amino acide residues at the active site of FGF2 which interact with heparin include: N27, R120, T121, K125, K129, Q134, K135, A136. It was observed from the docking study that even though the compounds interact with the binding site, the interaction between the compounds and the receptor was much lower than the native ligand, resulting in reduced inhibitory activity in comparison to the native ligand. Again, Figure 8 shows the docking interactions between compound nos. 10, 11 and 18 and the FGF2-FGFR1 complex. The interaction pattern thus determined was compared to those of the native ligand. Based on the docking results (Figure 8), it was observed that the compounds showed efficient activity as FGF2 stimulator because of their interaction with FGF2-FGFR1 complex. FGFR1 amino acids essential for interaction constitute of K160, K163, K172, K175, K177. Compound nos. 10, 18, and 11 showed hydrogen bond based interactions with Lys163 residue. However the degree of interaction of the compounds was less in comparison to the native ligand which showed hydrogen bond interactions with both Lys172 and Lys 177 amino acid residues. Therefore, the inhibitory activity of the studied compound was found to be lower than that of the native ligand. Based on docking interactions of the compounds with FGF2 and FGF2- FGFR1 complex, it could be concluded that compounds could act as stimulator of FGF2 signaling. Figure 9 shows the interactions of IGFR1 protein with compound nos. 12, 13 and 16 as well as the interactions for the native ligand. Based on the docking results (Figure 9), it was observed that the compounds did not show activity as IGFR1 inhibitor because the binding energy value was found to be greater than -4. The binding sites of IGF1R inhibitor include: 1005, 1007, 1079-1083, 1042; at which the native ligand indicated formation of two hydrogen bonds yet compound no. 13 showed only one hydrogen bond. Other compounds did not exhibit any hydrogen bond with the inhibitor binding site. Therefore, the compounds do not have inhibition activity against IGF1R. This results open the possibility that the compounds could fasten the proliferation phase and let IGF1 bind to IGF1R, initializing the proliferation signaling process.

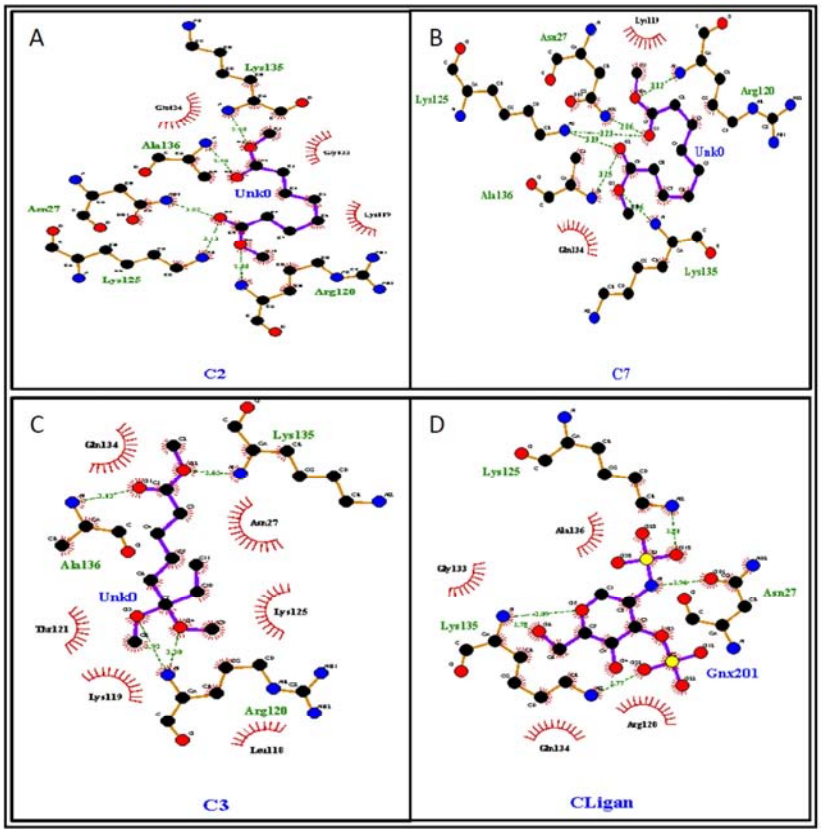

Figure 7. *2D interaction between compound with amino acid residue of FGF2 (A: compound number 2, B: compound number 8, C: compound number 3, D: ligand).*

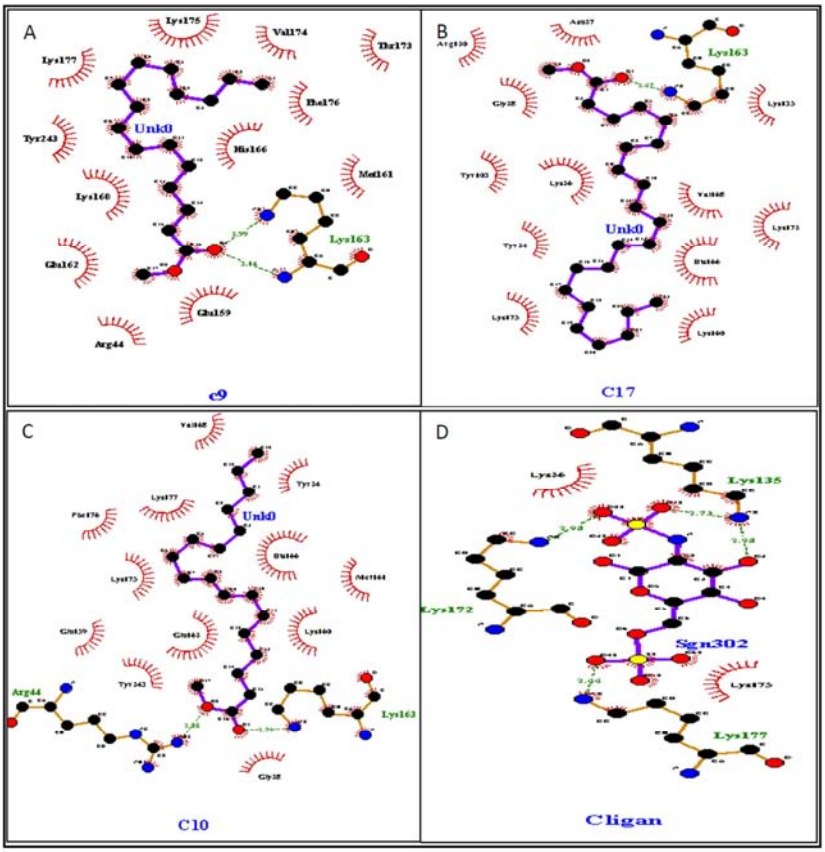

Figure 8. *2D interaction between compound with amino acid residue of FGF2-FGFR1 complex (A: compound number 10, B: compound number 18, C: compound number 11, D: ligand).*

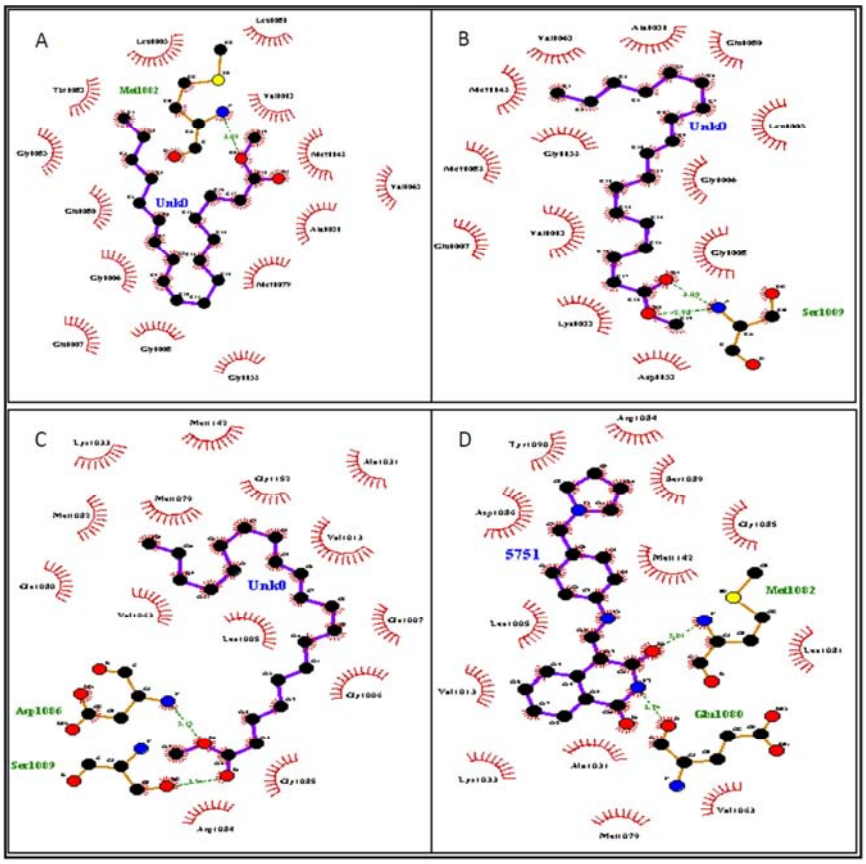

Figure 9. *2D interaction between compound with amino acid residue of IGF1R (A: compound number 13, B: compound number 16, C: compound number 12, D: ligand).*

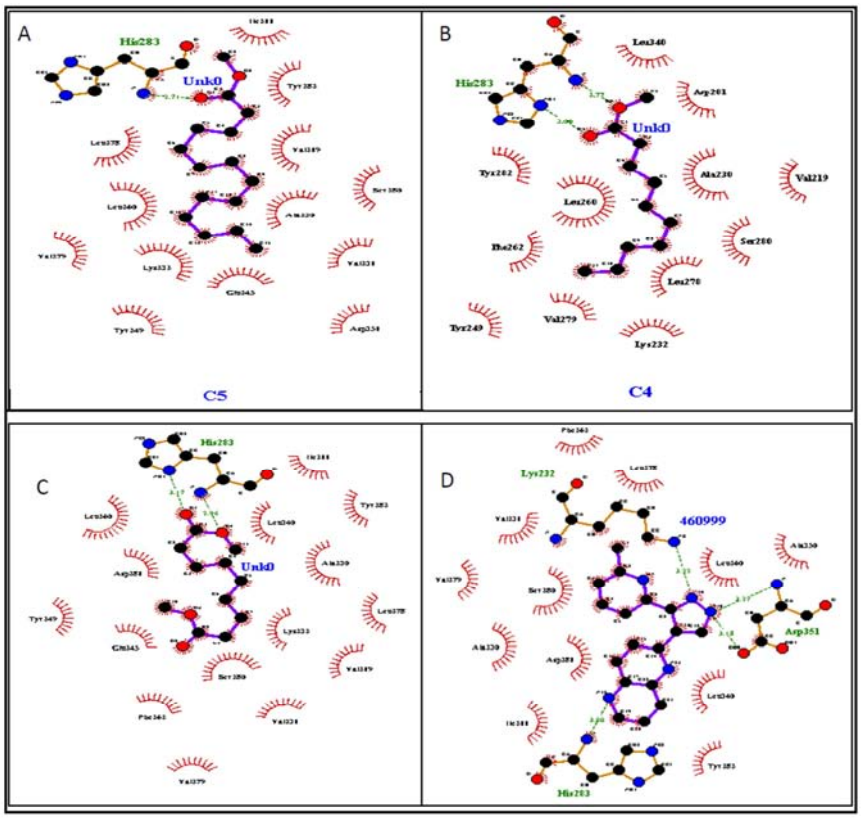

Figure 10. *2D interaction between compound with amino acid residue of TGF-β1 (A: compound number 6, B: compound number 4, C: compound number 8, D: ligand).*

3.3. Remodeling Phase

The results of docking studies related to the receptors involved in the remodeling phase are provided in Table 3. This stage constitutes the last phase of the wound healing process. Figure 10 shows the binding interactions of the amino acid residues of the TGF-β1 protein with compound nos. 4, 6, and 8 in addition to the interactions with the native ligand. Based on the docking results (Figure 10), it was observed that the compounds showed good activity as TGF-β1 inhibitor. Compared with the native ligand, the inhibition activity of the compounds were found to be half times lower than the native ligand because the native ligand showed three hydrogen bonds at Lys232, His238, Asp351 residues. On the contrary, the dalethyne derivatives showed only one hydrogen bond with His283 residue. The results showed that the TGF-β1 inhibitory activity of the compounds was minimum indicating that the compounds would not hinder the remodeling phase of the wound healing cycle.

In normal wound healing process, platelet activation occurs after wound appearance which in turn causes release of pro-inflammation cytokines such as TNF-α and IL-1β that will activate macrophage. Wound subsequently activates MMP-9 and COX-2 receptors. Further release of IL-1β and IL-6 inhibits fibroblast, keratinocyte proliferation and migration, which delays the epithelization and granulation process. The inhibition of fibroblast proliferation results in a decrease of FGF-2 synthesis and followed by a decrease in TGF-β1 expression regulation. This ultimately results in a decrease of the endothelial cell proliferation and therefore delays the neo- angiogenesis and vasculogenesis, resulting in a delay in the wound healing process. [24]. The molecular modeling studies infer that the in-house synthesized dalethyne derivatives that have been studied in the present work, bears the ability to inhibit the inflammation causing agents, MMP-9 and COX-2. On the other hand, the inability of the molecules to interact with the proteins hampering the proliferation of cells and re-epithelization further ensures the efficiency of the compounds to facilitate modulation of the expression of the growth factors (FGF-2 and TGF-β1) and inflammation mediators (IL-1β and IL-6), that aids the wound healing process.

4. Conclusion

The present work refers to the activity prediction of 18 dalethyne derivatives based on their interaction with the proteins that regulate the wound healing pharmacology of the human body. Subsequently all the molecules, synthesized in house, were docked with the various proteins involved in the process of wound healing and the binding energies of the molecules were calculated followed by prediction of their K_i values. For the validation of the docking methodology, the binding interactions of the molecules thus calculated were compared with that of the native ligand. In the normal wound healing process, platelet activation after the wound appearance causes the release of pro-inflammation cytokine such as TNF-α and IL-1β which will activate the macrophage. The wound will also activate MMP-9 and COX-2. The further release of IL-1β and IL-6 will inhibit the fibroblast production, keratinocyte proliferation and migration; which will delay the epithelization and granulation process. The inhibition of the fibroblast proliferation will cause the decrease of FGF-2 synthesis and therefore will also decrease the TGF- β1 expression regulation. This process will cause the decrease of endothelial cell proliferation and thus will delay the neoangiogenesis and vasculogenesis. At the same time, these phenomena will delay the wound healing process. In the present work, dalethyne derivatives have been predicted to have the ability to suppress the inflammation-causing agent, such as MMP-9 and COX-2. It could also lessen the increased oxidative stress and modulate the expression of the growth factors (FGF-2 and TGF-β1) and inflammation mediator (IL-1β and IL-6), which helps to fix the wound healing process.

In the purview of the pharmacology involved in the wound healing process, it was observed that the dalethyne derivatives showed effective interactions with the amino acid residues present in the active site of the proteins, MMP-9 and COX-2. This accounted for the conducive inhibitory effects of these molecules towards the respective receptors. Moreover, the simple structure of the dalethyne derivatives resembling the native ligand attributed to the inability to these molecules to bind with the proteins involved in the process of cell proliferation and re-epithelization. From these observations, it can thus be inferred that the dalethyne derivatives exhibited sufficient propensity to inhibit the inflammation-causing agents and at the same time allow unhindered execution of healing process. The results thus provide an insight for the structure of the dalethyne derivatives that would facilitate their activity as wound healing agents. Subsequently, the in house synthesized molecules can be suitably formulated into a pharmaceutical dosage form that can be efficiently used for the treatment of different types of wounds.

Acknowledgements

This study was sponsored and funded by the PT. Dermozone Pratama, Jakarta, Indonesia.

Conflict of Interest

The author has none to declare.

References

[1] S. A. Eming, T. Krieg, and J. M. Davidson (2007) Inflammation in wound repair: molecular and cellular mechanisms. Journal of investigative dermatology 127, 514-525.

[2] D. A. Enoch, H. A. Ludlam, N. M. Brown (2006) Invasive fungal infections: a review of epidemiology and management options. Journal of medical microbiology 55, 809-818.

[3] D. J. Leaper, and K. G. Harding, Wounds: biology and management. Oxford: Oxford University Press. 1998.

[4] G. Topman, N. Shoham, O. Sharabani-Yosef, F. H. Lin, A. Gefen (2013) A new technique for studying directional cell migration in a hydrogel-based three-dimensional matrix for tissue engineering model systems. Micron 51, 9-12.

[5] D. L. Epstein, L. L. Rowlett, and B. C. Roberts (1999) Acto-myosin drug effects and aqueous outflow function. Investigative Ophthalmology & Visual Science 40, 74–81.

[6] M. Kulac, C. Aktas, F. Tulubas, R. Uygur, M. Kanter, M. Erboga, M. Ceber, B. Topcu, O. A. Ozen (2013) The effects of topical treatment with curcumin on burn wound healing in rats Journal of Molecular Histology 44, 83-90.

[7] C. Mohanty, M. Das, and S. K. Sahoo (2012) Sustained wound healing activity of curcumin loaded oleic acid based polymeric bandage in a rat model. Molecular pharmaceutics 9, 2801-2811.

[8] M. Siavash, S. Shokri, S. Haghighi, M. A. Shahtalebi, Z. Farajzadehgan (2015) The efficacy of topical royal jelly on healing of diabetic foot ulcers: a double-blind placebo-controlled clinical trial. International wound journal 12, 137-142.

[9] M. Chen, H. Zheng, L. P. Yin, C. G. Xie (2010) Is oral administration of Chinese herbal medicine effective and safe as an adjunctive therapy for managing diabetic foot ulcers? A systematic review and meta-analysis. Journal of Alternative and Complementary Medicine 16, 889-898.

[10] J. W. Alexander, and D. M. Supp (2014) Role of arginine and omega-3 fatty acids in wound healing and infection. Advances in wound care (New Rochelle). 3, 682–690.

[11] T. Schultz, (2003) Quantitative Structure–Activity Relationships (QSARs) in Toxicology: A Historical Perspective. Journal of molecular structure: Theochem. 622, 1-22.

[12] T. Lengauer, and M, Rarey (1996) Computational methods for biomolecular docking. Current Opinion in Structural Biology 6, 402–406.

[13] A. Singh, A. Mishra, S. Verma, V. Purohit, R. K. Goel, (2014). Regulation of wound strength by Ocimum sanctum: in silico and in vivo evidences. International Journal of Basic & Clinical Pharmacology 3, 179-185.

[14] M. Incerti, L. Crascì, P. Vicini, E. Aki, I. Yalcin, T. Ertan-Bolelli, V. Cardile, A. C. E. Graziano, A. Panico (2018) Thiazolidinone derivatives as MMP inhibitors in tissue damage: Synthesis, biological evaluation and docking studies. Molecules 23, 415.

[15] A. Islam, M. S Hafez Kabir, R. Dash, T. B. Emran, M. Z. Uddin, K. Nesa, M. M. Nasir Uddin, M. T. Ahsan (2015). Virtual screening for potential COX-inhibiting constituents from *Mimosa pudica*. Journal of Applied Pharmaceutical Science 5, 71-75.

[16] K. S. Dharshan, (2018) Effect of +Dalethyne on Pseudomonas aeruginosa. Ijppr. Human. 12, 258-266.

[17] Ervina WF, A. D. W. Widodo and Y. P. Dahlan (2017) Pengaruh pemberian +dalethyne terhadap jumlah ekspresi il-1β pada tikus yang diinfeksi P. aeruginosa. Journal of Biosains Pascasarjana 19 (available online only).

[18] Marvin sketch (version. 6.0), 2013, ChemAxon (http://www.chemaxon.com).

[19] Protein Data Bank, www.rscb.org.

[20] Autodock 4.2, AutoDock Vina (http://vina.scripps.edu), 2006.

[21] PyMOL: The PyMOL Molecular Graphics System, Version 2.0 Schrödinger, LLC

[22] L. Koivisto, L. Hakkinen and H. Larjava, (2011) Re-epithelialization of wounds. Endodontic Topics, 24: 59–93.

[23] J. H. Wang, G. Yang, Z. Li, W. Shen (2004) Fibroblast responses to cyclic mechanical stretching depend on cell orientation to the stretching direction. J Biomechanics 37: 573–576.

[24] S. Guo, and L. A. Di Pietro (2010) Factors affecting wound healing. Journal of dental research 89, 219–229.